PHARMACIA

Pharmacia 71: 1–9
DOI 10.3897/pharmacia.71.e111178

Research Article

Preparation and characterization of vemurafenib microemulsion based hydrogel using surface active ionic liquid

Mohammed Jasim Neamah[1], Entidhar Jasim Muhammed Al-Akkam[1]

1 *Department of Pharmaceutics, College of Pharmacy, University of Baghdad, Baghdad, Iraq*

Corresponding author: Mohammed Jasim Neamah (phmohammedneamah@gmail.com)

Received 14 August 2023 ♦ **Accepted** 3 February 2024 ♦ **Published** 12 March 2024

Citation: Neamah MJ, Al-Akkam EJM (2024) Preparation and characterization of vemurafenib microemulsion based hydrogel using surface active ionic liquid. Pharmacia 71: 1–9. https://doi.org/10.3897/pharmacia.71.e111178

Abstract

Cancer is considered the second leading cause of death worldwide. Skin melanomas account for the highest mortality rate amongst all types of skin cancer. Systemic treatment with vemurafenib has a high rate of adverse effects, so attempts have been made to prepare a topical form of this drug. Microemulsions have been used to improve drug delivery to the skin. The microemulsions were prepared by dissolving vemurafenib in a mixture of peppermint oil and Smix, followed by the addition of water. The characteristics and effectiveness of surface-active ionic liquid-based vemurafenib microemulsions were characterised and evaluated in vitro. The vemurafenib microemulsions (CP5, CP7 and CP8) had droplet sizes in the microemulsion range (less than 200 nm), and they were used to prepare microemulsion-based hydrogels using HPMC K15M via the hot and cold method. The prepared microemulsion-based hydrogels were then evaluated. The microemulsion-based hydrogel GP5 exhibited higher skin deposition (45.4%) than the other hydrogels; thus, GP5 is a promising candidate for the topical treatment of melanoma by vemurafenib.

Keywords

Vemurafenib, microemulsion, surface-active ionic liquid

Introduction

Cancer is considered the second leading cause of death worldwide. Cancer accounts for 8 million deaths each year (Croce 2008). Skin cancer is a common type of cancer and includes squamous cell carcinoma, basal cell carcinoma and melanoma. Melanoma is not the most common type of skin cancer, but it is responsible for the highest number of fatalities amongst all types of skin cancer (Simoes et al. 2015). Vemurafenib is a drug that inhibits $BRAF^{V600E}$ kinase mutations. These mutations are common in human melanoma, and their inhibition will effectively inhibit the progression of melanoma (Flaherty et al. 2011). Systemic treatment with vemurafenib is accompanied with a high rate of adverse effects, so attempts were made to prepare a topical form of this drug to treat patients with melanoma and $BRAF^{V600E}$ kinase mutation (Almajidi et al. 2023). The skin is considered a suitable route for the topical delivery of drugs intended for local action, and microemulsion (ME) is one of the common drug delivery systems for the skin (Kutscher et al. 2015; Al-Rubaye and Al-Kinani 2023). MEs have received high interest because of their remarkable characteristics, which include the capacity to solubilise a wide range of drugs, low interfacial tension and large interfacial region. In addition, the formation of ME is continuous, and the preparation method is easy. ME is a nanoparticle system of two immiscible liquids. This system is stabilised by a film of surfactant, commonly with

co-surfactant, at the interface (Hejazifar et al. 2020). The most common type of surfactant used in ME is non-ionic surfactant, which has low toxicity. Non-ionic surfactants have several noticeable limitations when used in ME preparation. A high amount of non-ionic surfactants is needed for ME preparation and stabilisation. In addition, non-ionic surfactants have a restricted ability to dissolve extremely hydrophobic drugs (Madhav and Gupta 2011). Surface-active ionic liquids (SAILs) offer a good alternative to conventional non-ionic surfactants. SAILs show a better reduction in interfacial tension and more efficient stabilisation of the ME system compared with non-ionic surfactants. Ionic liquids are considered novel chemical compounds with extraordinary properties such as having no side products during production (it is considered a green and environment-friendly compound), low volatility and nonflammability. SAILs with imidazolium salts as the head group are the most predominant type of SAILs used in ME preparation (Gehlot et al. 2017).

This study aimed to prepare SAIL-based vemurafenib MEs and characterize them based on their particle size, polydispersity index (PDI) and zeta potential. The MEs were subjected to visual inspection and evaluated by centrifugation test, dilution test, electrical conductivity (EC) test, physical stability tests, pH, content uniformity test and in vitro drug release. The selected vemurafenib MEs were used to prepare ME-based hydrogels using HPMC K15M as a gelling agent. The prepared ME-based hydrogels were evaluated for their visual appearance, pH, spreadability, viscosity and rheology behaviour, ex vivo permeability, and skin deposition. An ME-based hydrogel that passes all these tests and has high skin deposition would be a potential dosage form for topical treatment of melanoma by vemurafenib.

Materials and methods

Materials

The materials used in this study were vemurafenib (Hangzhou Hyper Chemicals, China), peppermint oil (BAR_SUR_LOUP, France), PEG 400 (Vardaan House, India), 1-tetradecyl-3-methylimidazolium bromide (C14MIB) and HPMC K15M (Hyperchem, China), potassium dihydrogen phosphate, disodium hydrogen phosphate and hexadecyltriammonium bromide (HTAB; Hejazifar et al. 2020; Himedia, India).

Construction of pseudoternary phase diagram

Phase behaviour study was conducted to estimate the ME area and predict the quantities of each SAIL (C14MIB), co-surfactant (PEG 400) and oil (peppermint oil) used to prepare a stable ME. The procedure included using different SAIL: co-surfactant (Smix) ratios, including 1:2, 1:3 and 1:4 w/w. Each of the previously mentioned Smix ratios was mixed separately with peppermint oil in different weight ratios (i.e. 1:9, 2:8, 3:7, 4:6, 5:5, 6:4, 7:3, 8:2 and 9:1 w/w). Water was added to each oil: Smix ratio with gentle stirring until turbidity appeared. The amount of water (in gm) added in each oil: Smix ratio was recorded, and the weight percent of each oil: Smix: water was recorded and used to prepare the pseudoternary phase diagram (Maraie and Almajidi 2018; Farooq et al. 2019).

Preparation of microemulsion

MEs were prepared by dissolving 10 mg of vemurafenib in a different mixture of peppermint oil and Smix and stirred until the drug was completely dissolved in the oil: Smix mixture. Subsequently, the required amount of water was added dropwise for 10 min until a homogenized translucent mixture was achieved. The prepared formulas were left for 24 h to equilibrate (Naeem 2019). Nine formulas (CP1–CP9) were prepared using Smix ratios of 1:4, 1:3 and 1:2. Formulas CP1, CP2 and CP3 were prepared using a Smix ratio of 1:4. Formulas CP4, CP5 and CP6 were prepared using a Smix ratio of 1:3. Formulas CP7, CP8 and CP9 were prepared using a Smix ratio of 1:2. Formulas CP3, CP6 and CP9 were prepared using 15% w/w peppermint oil, whereas other formulas contained 10% w/w peppermint oil. Formulas CP2, CP5 and CP8 contained 70% w/w Smix, and other formulas contained 60% w/w Smix (Table 1).

Table 1. Composition of different vemurafenib microemulsions.

Formula No.	Smix ratio	Percent of each ingredient			
		Vemurafenib % w/w	Peppermint oil % w/w	Smix % w/w	Water % w/w
CP1	1:4	0.2	10	60	30
CP2		0.2	10	70	20
CP3		0.2	15	60	25
CP4	1:3	0.2	10	60	30
CP5		0.2	10	70	20
CP6		0.2	15	60	25
CP7	1:2	0.2	10	60	30
CP8		0.2	10	70	20
CP9		0.2	15	60	25

Measurement of particle size, PDI and zeta potential

The Zetasizer apparatus (Malvern, the UK) was used to measure the particle size and PDI for all formulas (CP1–CP9). About 1 mL of each sample was obtained and diluted up to 3 mL with deionized distilled water (to ensure that sample viscosity was comparable with water viscosity and facilitate free movement of ME particles). The diluted formulas were placed in the instrument, and the particle size and PDI were recorded for each formula (Basheer et al. 2013; Sukre et al. 2022). Zeta potential was measured using the same instrument, and only formulas that passed all tests were used to prepare ME-based hydrogels.

Visual inspection and centrifugation test

MEs were examined visually to confirm their translucency and the absence of any turbidity or coalescence. Thereafter, the prepared MEs were subjected to centrifugation at 3000 rpm for 5 min and examined for any separation or turbidity to confirm that the prepared MEs could withstand vigorous shear stresses.

Dilution test

Dilution tests were performed to predict whether the prepared ME was o/w or w/o and could be diluted in a gel base. This test was performed by adding deionised distilled water to 1 mL of each prepared formula, and their clarity and the absence of any turbidity were observed (Nirmala et al. 2013).

EC test

EC was measured using a conductivity meter (TDS Ec Meter Temperature Tester, China) by placing the device electrode in the prepared SAIL-based MEs. The electrical current was recorded and measured in μS/cm (Changmai et al. 2019).

Physical stability tests

The physical stability of the MEs was determined through two tests. The first test was called the heating–cooling cycle. In this test, the prepared SAIL-based ME was subjected to different temperatures (4 °C, 25 °C and 40 °C) for at least 48 h for each temperature. The second test called the freeze–thaw cycle included storage of the prepared SAIL-based ME at -20 °C and 25 °C for 48 h at each temperature. This cycle was repeated three times. Thereafter, the MEs were inspected for any possible turbidity or separation (Bergonzi et al. 2014; Ghareeb 2020).

pH measurement

pH was measured using a pH meter device (HANNA RI 02895, Romania). The instrument was calibrated at pH 7 and 4 using standard buffer solutions. The probe of the device was dipped in each prepared ME (CP1–CP9), and the resultant pH was recorded (Sukre et al. 2022).

Content uniformity test

The drug content of each prepared SAIL-based ME (100 mg) was determined by diluting it with methanol to a concentration that could be detected spectrophotometrically (10 mL) and measuring the concentration at λ_{max} 305 nm (Yadav et al. 2017). The drug content of each formula was measured using the actual and theoretical drug contents via the following equation:

$$\text{Drug content}\,(\%) = \frac{\textit{Actual drug content}}{\textit{Theoretical drug content}} * 100\% \qquad (1)$$

In vitro drug release

In vitro drug release was determined using the dialysis bag method. The dialysis bag had a pore size between 8,000 and 12,000 Da. The dissolution medium was the same FDA dissolution medium of vemurafenib that consisted of 1% HTAB (Hejazifar et al. 2020) in 0.05 M phosphate buffer, pH 6.8. The procedure included hydration of the dialysis bag with the previously mentioned dissolution medium for 24 h. Thereafter, 1 g of each formula was placed in the hydrated dialysis bag and sealed from each side. The loaded dialysis bag was placed in 100 mL of dissolution medium and rotated at 50 rpm at 37 °C. About 3 mL of sample was withdrawn from the dissolution medium after 1, 2, 4, 6, 12 and 24 h. Vemurafenib absorbance was measured at λ_{max} 307 nm, and the concentration of vemurafenib in each sample was estimated using a calibration curve equation. The percent of the cumulative amount released was predicted from the estimated concentration (Huang et al. 2008; Dawood et al. 2018).

Preparation of ME-based hydrogel

The ME-based hydrogels were prepared using HPMC K15M as the gelling agent. The required amount of HPMC K15M was gradually added to boiled deionised water while stirring at 15000 rpm. The concentration of HPMC K15M prepared was 5% and 7% w/v HPMC K15M. The selected formula of the cold MEs (CP5, CP7 and CP8) was added to the prepared boiled HPMC K15M mixture in a ratio of 1:1 w/w with continuous stirring. The prepared ME-based hydrogels were stored in the refrigerator for 24 h for complete relaxation and gel formation (El-Say et al. 2016). Six formulas (GP1–GP6) of ME-based hydrogels were prepared. The ME used in GP1 and GP2 was from CP5. The ME used in GP3 and GP4 was from CP7, and the ME used in GP5 and GP6 was from CP8 (Table 2).

Visual appearance

ME-based hydrogels (GP1–GP6) were inspected for their transparency (or translucency), homogeneity, general consistency and phase separation (Almajidi et al. 2022).

pH measurement

pH was measured using a pH meter device (HANNA RI 02895, Romania). The instrument was calibrated at pH 7 and 4 using standard buffer solutions. The probe of the device was dipped in each prepared ME-based hydrogel (GP1–GP6), and the resultant pH was recorded (Jaber et al. 2020).

Spreadability test

The parallel plate method was used to estimate the spreadability of ME-based hydrogels. About 1 g of each prepared ME-based hydrogel (GP1–GP6) was placed on the centre of a glass plate (20×20 cm) that was placed on white paper.

Table 2. Composition of the different microemulsion-based hydrogels.

Formula No.	HPMC 5% (Changmai et al. 2019)	HPMC 7% (Changmai et al. 2019)	Formula CP5 (Changmai et al. 2019)	Formula CP7 (Changmai et al. 2019)	Formula CP8 (Changmai et al. 2019)
GP 1	4	–	4	–	–
GP 2	–	4	4	–	–
GP 3	4	–	–	4	–
GP 4	–	4	–	4	–
GP 5	4	–	–	–	4
GP 6	–	4	–	–	4

Another glass plate of the same size was placed on the first plate, and a 2 kg weight was placed on the second plate. The sample was allowed to spread between the two plates for a few minutes until no further spreading was expected (Jaber et al. 2020). The spreadability capacity (g·cm/s) was measured using the following equation:

$$Spreadability\left(g\cdot\frac{cm}{sec}\right)=\frac{weight\ placed\ (gm)\times\ length\ of\ sample\ migration\ (cm)}{Time\ (sec)} \quad (2)$$

Viscosity and rheology studies

A viscosity and rheology study was conducted by using a Brookfield digital viscometer (NDJ–5S). The spindle (spindle No. 4) of the device was placed in each ME-based hydrogel prepared (GP1–GP6) and rotated at different speed rates (6, 12, 30 and 60 rpm) for 30 s at each speed. The viscosity was recorded at each speed (Sabri et al. 2009).

Ex vivo permeability study

The skin permeability study was performed using the abdominal skin of Wister Albino rats with the University of Baghdad–College of Pharmacy ethics committee. The experiment was performed using Copley® Franz cell (Nottingham, the UK). The receptor cell was filled with FDA dissolution media of vemurafenib (1% HTAB in 0.05 M phosphate buffer, pH 6.8), and skin was placed on the top of the receptor cell. The skin's outer layer was facing the donor compartment, and the inner part was facing the receptor part of the cell. A ring (whose cavity had a surface area of 1.76 cm^2) was placed on the skin's outer layer. About 200 mg of hydrogel was placed in the ring orifice and spread uniformly. The system was sealed by placing a cover and sprig above the ring to prevent any contamination of the sample. The prepared Franz cell was placed in the device that kept the temperature at 37 °C and rotated at 50 rpm. The samples (1 mL) were collected at a predetermined time (after 1, 2, 4, 6, 12 and 24 h) (Bayoumi et al. 2022). Vemurafenib absorbance was measured at 307 nm, and the concentration of vemurafenib in each sample was estimated using the calibration curve equation. The cumulative amount released was calculated and divided by surface area to determine the cumulative amount released per area.

Ex vivo skin deposition study

After skin permeability as finished, the skin of each ME-based gel (GP1–GP6) was washed with 7.8 phosphate buffer many times to remove any gel on the surface of the skin. The skin was cut into small pieces and immersed in up to 10 mL of methanol and sonicated for a few minutes. The sample was centrifuged at 6000 rpm for 10 min, and the absorbance of vemurafenib was measured spectrophotometrically at 305 nm. Skin deposition was measured using the following equation (Fan et al. 2013):

$$Skin\ deposition\ (\%)=\frac{Actual\ drug\ content}{Theoretical\ drug\ content}*100\% \quad (3)$$

Statistical analysis

Statistical analysis for all experimental data was performed using IBM SPSS Statistic 25 software. Data were expressed as the mean values with their standard deviation (SD). ANOVA with post hoc test was used to approve the significance between results with $P < 0.05$. The DDsolver program was applied to detect the kinetics of drug release.

Results and discussion

Pseudoternary phase diagram

Pseudoternary phase diagram construction is regarded as a simple and efficient method to predict the effect of different compositions of oil and Smix on the ME system. Fig. 1 represents the pseudoternary phase diagram of different Smix ratios against peppermint oil and water. Fig. 1A–C represent the pseudoternary phase diagram when the Smix ratio used was 1:2, 1:3 and 1:4, respectively. The shaded area in the previously mentioned figure represented the two-phase or macroemulsion area, and the remaining white area represented the one-phase or ME area. The pseudoternary diagrams revealed that the ME area increased when the Smix ratio rose from 1:4 to 1:2. These

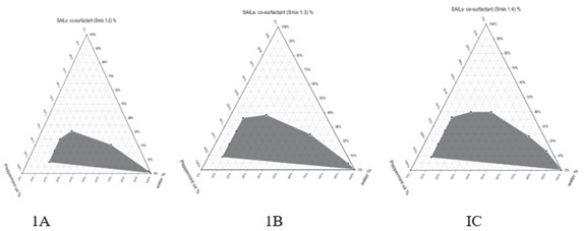

Figure 1. Pseudoternary phase diagram. **A–C.** Represent the pseudoternary phase diagram at the Smix ratios of 1:2, 1:3 and 1:4, respectively.

results indicated that increasing the fraction of SAILs to PEG 400 in the Smix mixture increased the quantity of water held in the ME mixture and increased the ME or one-phase area. These observations agreed with the research, which mentioned that SAILs have superior surface activity to conventional non-ionic surfactants and co-surfactants that result in dramatically decreased surface tension (Ali et al. 2019; Hammodi and Abd Alhammid 2020).

Particle size and PDI of vemurafenib ME

The average particle size and PDI of all prepared SAIL-based formulas are listed in Table 3. When comparing formulas with the same Smix ratios and Smix % but with differences in the percent of peppermint oil, CP1 had an average particle size of 249.8 ± 3.7 nm, whereas CP 3 had an average particle size of 959.6± 16.9 nm. Similarly, a significant increase ($P < 0.05$) was observed in the average particle size between CP6 (that had 15% of peppermint oil and average particle size of 456.6 ± 31.3 nm) and CP4 (that contained 10% of peppermint oil and average particle size of 237.0 ± 3.7 nm). The same trend was found when comparing the particle size of CP7 and CP9. These observations could be explained by the fact that increasing the percentage of oils in the prepared MEs could increase the swelling and size of ME particles (Chrismaurin et al. 2023).

Increasing the concentration of Smix (while keeping the Smix ratio constant) from 60% in CP1 to 70% in CP2 decreased the particle size from 249.8 ± 3.7 nm in CP1 to 171.3 ± 3.6 nm. The same observation was found with CP4 (with 60% of Smix and average particle size of 237.0 ± 3.7 nm) and CP5 (with 70% of Smix and average particle size of 11.4 ± 1.15 nm). These observations continued when the average particle size of CP7 (with 70% of Smix and average particle size of 58.1 ± 1.3 nm) was compared with that of CP8 (with 70% of Smix and average particle size of 5.2 ± 0.4 nm). Increasing the quantity or percent of Smix in the formulas could decrease the surface tension and dramatically decrease the free energy needed to break down the ME droplets into small particles (Sarheed et al. 2020; Hamed and Abd Alhammid 2021).

Moreover, increasing the quantity of SAILs in the Smix ratio by reserving the Smix percent in the formulas decreased the particle size of the prepared SAIL-based MEs. For example, CP2 (with Smix ratio of 1:4 w/w) had an average particle size of 171.3 ± 3.6 nm, CP5 (with Smix ratio of 1:3 w/w) had an average particle size of 11.4 ± 1.15 nm and CP8 (with Smix ratio of 1:2 w/w) had an average particle size of 5.2 ± 0.4 nm. All these formulas had the same Smix percent of 70%, but they differed in the quantity or ratio of SAILs in the Smix in these formulas. These observations led to the prediction that increasing the ratio of SAILs in Smix could significantly decrease the particle size of the prepared ME droplets and prove the superiority of SAILs in decreasing the interfacial tension and the surface free energy to break the ME droplets to small droplets.

Visual inspection and centrifugation results of vemurafenib MEs

All the prepared SAIL formulas were yellow translucent formulas with no signs of turbidity or separation. In addition, all formulas passed the centrifugation test without any separation, coalescence, or turbidity.

Dilution test results

All formulas that had 15% of peppermint oil (CP3, CP6 and CP9) failed to pass the dilution test and showed turbidity when diluted. All formulas with a Smix ratio of 1:4 failed the dilution test (CP1, CP2 and CP3). Only one formula (CP5) with a Smix ratio of 1:3 passed the dilution test. CP7 and CP8 with Smix ratio of 1:2 passed the dilution test. Results from the dilution test are listed in Table 3.

EC of vemurafenib ME

EC is an important test to predict the type of MEs whether they are o/w or w/o type. The o/w MEs, in which water was the continuous phase, had water channels that were capable of carrying electrical current. All the prepared SAIL-based MEs (CP1–CP9) had electrical charge. These observations proved that the prepared MEs were o/w type (Table 3; El Agamy and El Maghraby 2015).

pH measurement of vemurafenib ME

All the prepared SAIL-based MEs (CP1–CP9) had a pH range of 4.51 ± 0.18 to 5.86 ± 0.05. This pH range is ac-

Table 3. Particle Size, PdI, dilution test, electrical conductivity, pH and drug content of vemurafenib microemulsions.

Formula No.	Particle size (nm)	PdI	Dilution test	Electrical conductivity (µs/cm)	pH	Drug content (%)
CP 1	249.8 ± 3.7	0.3867 ± 0.03	Failed	540 ± 22	5.35 ± 0.04	99.3 ± 0.4
CP 2	171.3 ± 3.6	0.3837 ± 0.05	Failed	626 ± 38	5.28 ± 0.03	99.6 ± 0.3
CP 3	959.6 ± 16.9	0.37 ± 0.06	Failed	353 ± 8	4.69 ± 0.07	99.4 ± 0.2
CP 4	237.0 ± 3.7	0.27 ± 0.04	Failed	568 ± 52	5.36 ± 0.06	99.2 ± 0.3
CP 5	11.4 ± 1.15	0.39 ± 0.07	Passed	671 ± 26	5.45 ± 0.04	99.3 ± 0.4
CP 6	456.6 ± 31.3	0.37 ± 0.14	Failed	341 ± 10	4.77 ± 0.04	99.5 ± 0.3
CP 7	58.1 ± 1.3	0.25 ± 0.05	Passed	523 ± 10	5.57 ± 0.09	99.1 ± 0.4
CP 8	5.2 ± 0.4	0.35 ± 0.08	Passed	543 ± 27	5.86 ± 0.05	99.3 ± 0.3
CP 9	459.0 ± 24.6	0.41 ± 0.06	Failed	325 ± 27	4.51 ± 0.18	98.9 ± 0.8

(Results expressed as mean ±SD, n=3)

ceptable for topical preparations that have a gentle effect on the skin without irritation. The pH of formulas that had 10% of peppermint oil (containing high percentage of Smix), which included formulas CP1, CP2, CP4, CP5, CP7 and CP8, was significantly higher than the pH of formulas with 15% of peppermint oil (containing low percent of Smix), which included formulas CP3, CP6 and CP9 (Table 3).

Content uniformity of vemurafenib ME

The drug contents for different SAIL-based MEs (CP1–CP9) are listed in Table 3 and ranged from 99.5 ± 0.3% to 98.9 ± 0.8%. The US Pharmacopeia accepts formulas or dosage forms with drug content percentages ranging from 85% to 115%. Hence, all the prepared MEs had drug contents within the acceptable range (Hammodi and Abd Alhammid 2020).

In vitro drug release of vemurafenib ME

The release profiles of different prepared SAIL-based MEs (CP1–CP9) are shown in Fig. 2. All formulas (CP1–CP9) showed excellent release profiles with cumulative release percentages within the acceptable range within 24 h.

The kinetics of the vemurafenib release profile from each SAIL-based ME (CP1–CP9) was instigated using the DDsolver program. All formulas showed a first-order release profile with R^2 ranging from 0.994 to 0.999. Table 4 shows the fit of the SAIL-based ME (CP1–CP9) to different kinetics of drug release including zero-order, first-order and Higuchi kinetics.

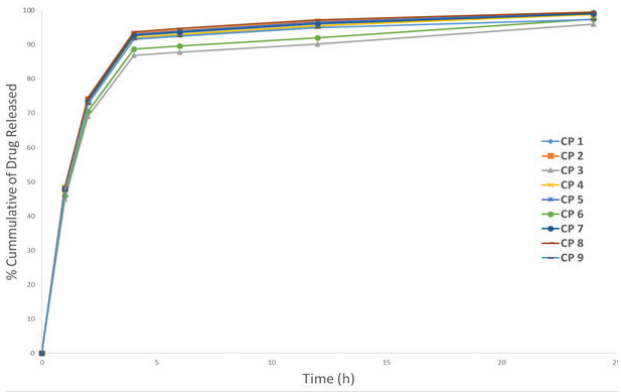

Figure 2. Release profile of vemurafenib from different SAIL-based microemulsion formulas.

Table 4. Rate kinetic and R2 for different order kinetics for SAIL-based microemulsions.

Formula No.	Order					
	Zero-order		First order		Higuchi	
	K_0	R^2	K_1	R^2	K_H	R^2
CP 1	5.986	0.620	0.552	0.994	28.166	0.823
CP 2	6.011	0.605	0.649	0.999	28.378	0.813
CP 3	5.719	0.634	0.552	0.994	26.819	0.833
CP 4	5.970	0.614	0.641	0.999	28.132	0.819
CP 5	6.015	0.610	0.657	0.999	28.363	0.817
CP 6	5.823	0.630	0.582	0,996	27.331	0.830
CP 7	5.997	0.612	0.651	0.999	28.271	0.817
CP 8	6.044	0.606	0.670	0.999	28.528	0.814
CP 9	5.910	0.608	0.632	0.998	27.883	0.815

Selection of best vemurafenib me

The prepared SAIL-based MEs (CP5, CP7 and CP8) had passed all ME characterization and evaluation tests and had droplet size in the ME range (less than 200 nm), were used to prepare me-based hydrogel using HPMC K15M as a gelling agent using the hot and cold method.

Visual appearance, pH and spreadability of ME-based hydrogels

All the prepared hydrogels (GP1–GP6) were yellow, clear and translucent. No signs of creaming or gel separation were detected. The results of the pH and spreadability test of the prepared hydrogels (GP1–GP6) are listed in Table 5. The pH ranged from 5.00 ± 0.11 to 5.43 ± 0.06, which was acceptable for topical preparations with no risk of skin irritation. We observed a significant difference in the spreadability of different prepared gels, which may be attributed to the difference in their viscosity.

Viscosity and rheology study

Each of the prepared ME-based hydrogels (GP1–GP6) was subjected to different shear rates ranging from 1.32 s^{-1} to 1326 s^{-1}. All the hydrogels (GP1–GP6) showed decreasing viscosi-

Table 5. pH, spreadability, viscosity, Jss, Tlag, Kp, VEM permeated in 24 h (%) and skin deposition (μg) of different microemulsion-based hydrogels.

Formula No.	pH	Spreadability (gm· cm/s)	Viscosity (mPa·s) at 6 rpm	Jss (μg/cm²·h)	T_{lag} (Flaherty et al. 2011)	K_p (cm/h)	VEM permeated in 24 h (%)	Skin deposition (%)
GP 1	5.43 ± 0.06	91.1 ± 1.76	2747 ± 106	1.0594	0.7659	0.001059	21.5	20.5 ± 0.7
GP 2	5.24 ± 0.08	90.1.3 ± 1.38	4613 ± 161	0.9535	0.851	0.000954	19.3	18.5 ± 0.5
GP 3	5.03 ± 0.11	71.34 ± 2.13	24465 ± 105	1.6546	4.4172	0.001655	31.3	26.7 ± 0,4
GP 4	5.01 ± 0.11	68.2 ± 1.05	46098 ± 260	1.6417	5.9369	0.001642	30.3	24.4 ± 0.6
GP 5	5.21 ± 0.10	88.8 ± 3.13	13684 ± 132	2.7026	8.3481	0.002703	49.2	45.4 ± 0.2
GP 6	5.00 ± 0.11	75.15 ± 2.03	34000 ± 117	1.8918	5.8437	0.001892	34.5	32.0 ± 0.8

(Results expressed as mean ±SD, *n*=3).

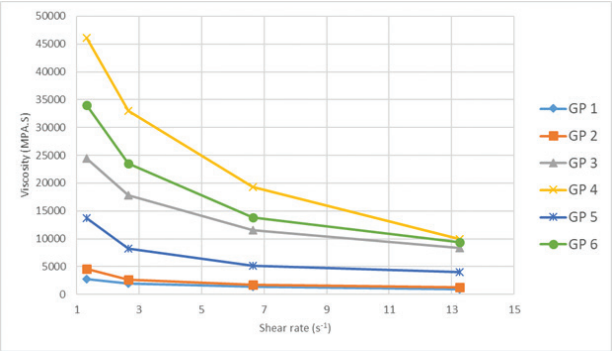

Figure 3. Rheological behaviour of different microemulsion-based hydrogel formulas.

ty upon increasing shear rate (Fig. 3). These results indicated the pseudoplastic behaviour of the hydrogels (GP1–GP6), which could be explained by a temporary breakdown of the complex structure of the polymer linkage and alliance of the polymer layer in a regular manner (Lim et al. 2015; Ferreira et al. 2016). The gel's pseudoplastic behaviour facilitated the improved spread on the skin upon application.

Ex vivo permeability

The cumulative amount permeated per square centimetre versus the time of different ME-based hydrogel formulas is shown in Fig. 4. We compared the vemurafenib flux (Jss) and permeability coefficients (Flaherty et al. 2011; Table 5) of GP1 and GP2 (which were prepared from the same microemulsion CP5). As shown in Table 5, GP1 had significantly higher ($P < 0.05$) J_{ss} and K_p than GP2. This observation could be attributed to the lower viscosity (2747 ± 106 mP·s at 6 rpm) of the prepared GP1 gel compared with the viscosity of GP2 gel (4613 ± 161 mP·s at 6 rpm). The high viscosity of the gel delayed the release of vemurafenib from the gel base, so the release of vemurafenib from the gel was inversely proportional to the gel viscosity. Similar results

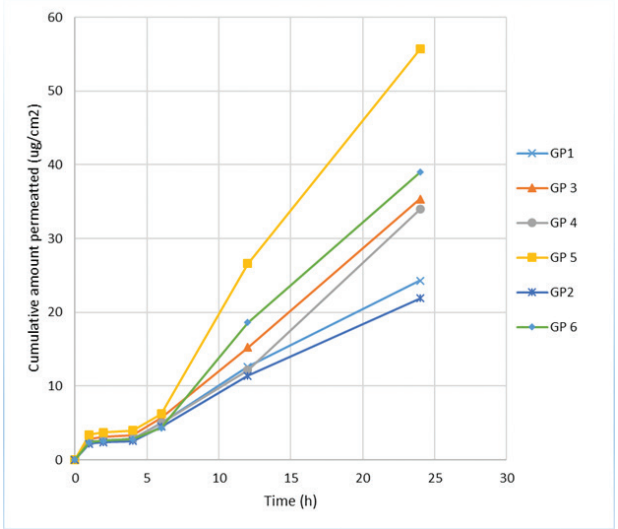

Figure 4. Cumulative amount permeated per square centimetre versus time of different microemulsion-based hydrogel formulas.

were found when comparing the permeability profile of GP3 (24465 ± 105 mP·s at 6 rpm) and GP4 (46098 ± 260 mP·s at 6 rpm) where both of these prepared gels were prepared from the same ME (CP7), as well as when comparing the permeability profile of GP3 (13684 ± 132 mP·s at 6 rpm) and GP4 (34000 ± 117 mP·s at 6 rpm) where these prepared gels were prepared from the same ME (CP8).

In addition, J_{ss} and K_p were affected by the Smix ratio and percent present in the ME used to prepare different hydrogels. Formulas containing a higher SAIL percent had J_{ss} and K_p when compared with the other prepared gels. Thus, GP5 and GP6 (with SAIL approximately 33% of Smix and % Smix 70% w/w) had significantly higher J_{ss} and K_p compared with GP1 and GP2 (with SAIL 25% of Smix and % Smix 70% w/w). Similarly, GP6 hydrogel (with SAILs 25% of Smix and % Smix 60 % w/w) had significantly higher J_{ss} and K_p compared with GP3, even though GP3 had lower viscosity (24465 ± 105 mP·s at 6 rpm) than GP6 (34000 ± 117 mP·s at 6 rpm). This elevation in J_{ss} and K_p can be explained by the number of SAILs present in GP6 when compared with those in GP3. SAILs acted as permeability enhancers. Hydrophilic SAIL-like C14MIB can break the tight junction present in the skin, thereby increasing the paracellular transport of vemurafenib through skin (Agatemor et al. 2018).

Skin deposition tests were performed as the prepared vemurafenib-based hydrogels was used for topical treatment of skin melanoma. Amongst the tested formulas, GP5 had the highest skin deposition rate (45.4% ± 0.2%; Table 5).

Conclusion

The topical delivery of vemurafenib is a promising route of drug administration to skin melanoma. MEs were used to enhance drug penetration to the skin. SAILs dramatically increased the water content of the MEs and decreased the particle size of ME droplets. The penetration of ME droplets was increased by increasing the quantity of SAILs in the formula because SAILs acted as permeation enhancers. ME-based hydrogel GP5 had the highest skin deposition (45.4%) amongst the tested hydrogels, suggesting its suitability as a possible formulation for the topical treatment of melanoma by vemurafenib.

Acknowledgments

The authors thank the College of Pharmacy – University of Baghdad for their support and for providing the necessary facilities to complete this research.

The committee protocol in the College of Pharmacy/ University of Baghdad approved this study (No: REACUBCP33023A), which complied with the guideline for the Care and Use of Laboratory Animals published by the US National Institutes of Health (NIH Publication No 85–23, revised 1996).

References

Agatemor CKN, Ibsen EET, Mitragotri S (2018) Ionic liquids for addressing unmet needs in healthcare. Bioengineering & Translational Medicine 3(1): 7–25. https://doi.org/10.1002/btm2.10083

Al-Rubaye RA, Al-Kinani KK (2023) Formulation and evaluation of prednisolone acetate microemulsion ocular gel. The Egyptian Journal of Hospital Medicine 90(1): 1744–1751. https://doi.org/10.21608/ejhm.2023.284303

Ali MK, Moshikur RM, Wakabayashi R, Tahara Y, Moniruzzaman M, Kamiya N, Goto M(2019) Synthesis and characterization of choline–fatty-acid-based ionic liquids: A new biocompatible surfactant. Journal of Colloid and Interface Science 551: 72–80. https://doi.org/10.1016/j.jcis.2019.04.095

Almajidi YQ, Maraie NK, Raauf AM (2022) Modified solid in oil nanodispersion containing vemurafenib-lipid complex-in vitro/in vivo study. F1000Research 11: 841. https://doi.org/10.12688/f1000research.123041.2

Almajidi YQ, Maraie NK, Raauf AM (2023) Utilization of solid in oil nanodispersion to prepare a topical vemurafenib as potential delivery system for skin melanoma. Applied Nanoscience 13(4): 2845–2856. https://doi.org/10.1007/s13204-024-03024-3

Basheer HS, Noordin MI, Ghareeb MM (2013) Characterization of microemulsions prepared using isopropyl palmitate with various surfactants and cosurfactants. Tropical Journal of Pharmaceutical Research 12(3): 305–310. https://doi.org/10.4314/tjpr.v12i3.5

Bayoumi SA, Dawaba AM, Zalat ZA, Ammar AA (2022) Formulation and evaluation of HPMC topical gel of Ectoine. Azhar International Journal of Pharmaceutical and Medical Sciences 2(2): 60–69. https://doi.org/10.21608/aijpms.2022.94549.1092

Bergonzi MC, Hamdouch R, Mazzacuva F, Isacchi B, Bilia AR (2014) Optimization, characterization and in vitro evaluation of curcumin microemulsions. LWT-Food Science and Technology 59(1): 148–155. https://doi.org/10.1016/j.lwt.2014.06.009

Changmai, A, Adhikari A, Dey BK (2019) Preparation and evaluation of Microemulsion containing clove oil and peppermint oil as active compound. Journal of Pharmaceutical and Scientific Innovation 8(4): 155–158. https://doi.org/10.7897/2277-4572.084145

Chrismaurin F, Dwiastuti R, Chabib I, Yuliani SH (2023) The effect of olive oil, tween 60 and span 20 on physical characteristics of quercetin nanoemulgel. International Journal of Applied Pharmaceutics 15(1): 212–217. https://doi.org/10.22159/ijap.2023v15i1.46423

Croce CM (2008) Oncogenes and cancer. New England Journal of Medicine 358(5): 502–511. https://doi.org/10.1056/NEJMra072367

Dawood NM, Abdul-Hammid S, Hussein A (2018) Formulation and characterization of lafutidine nanosuspension for oral drug delivery system. International Journal of Applied Pharmaceutics 10(2): 20–30. https://doi.org/10.22159/ijap.2018v10i2.23075

El-Say KM, Abd-Allah FI, Lila AE, Hassan AE-SA, Kassem AEA (2016) Diacerein niosomal gel for topical delivery: development, in vitro and in vivo assessment. Journal of Liposome Research 26(1): 57–68. https://doi.org/10.3109/08982104.2015.1029495

El Agamy HI, El Maghraby GM (2015) Natural and synthetic oil phase transition microemulsions for ocular delivery of tropicamide: efficacy and safety. Journal of Applied Pharmaceutical Science 5(2): 067–075. https://doi.org/10.7324/JAPS.2015.58.S11

Fan C, Li X, Zhou Y, Zhao Y, Ma S, Li W, Liu Y, Li G (2013) Enhanced topical delivery of tetrandrine by ethosomes for treatment of arthritis. BioMed Research International 2013: e161943. https://doi.org/10.1155/2013/161943

Farooq SU, Kumar DS, Shahid AA (2019) Formulation and evaluation of vitamin D3 (Cholecalciferol) self-nanoemulsifying drug delivery systems for enhancing solubility. International Journal of Pharmacy and Biological Sciences 9(3): 587–598.

Ferreira SBDS, Moço TD, Borghi-Pangoni FB, Junqueira MV, Bruschi ML (2016) Rheological, mucoadhesive and textural properties of thermoresponsive polymer blends for biomedical applications. Journal of the Mechanical Behaviour of Biomedical Materials 55: 164–178. https://doi.org/10.1016/j.jmbbm.2015.10.026

Flaherty KT, Yasothan U, Kirkpatrick P (2011) Vemurafenib. Nature reviews Drug Discovery 10(11): 811–812. https://doi.org/10.1038/nrd3579

Gehlot PS, Kulshrestha A, Bharmoria P, Damarla K, Chokshi K, Kuma A (2017) Surface-active ionic liquid cholinium dodecylbenzenesulfonate: self-assembling behaviour and interaction with cellulase. ACS Omega 2(10): 7451–7460. https://doi.org/10.1021/acsomega.7b01291

Ghareeb MM (2020) Formulation and characterization of isradipine as oral nanoemulsion. Iraqi Journal of Pharmaceutical Sciences 29(1): 143–153. https://doi.org/10.31351/vol29iss1pp143-153

Hamed SB, Abd Alhammid SN (2021) Formulation and characterization of felodipine as an oral nanoemulsions. Iraqi Journal of Pharmaceutical Sciences 30(1): 209–217. https://doi.org/10.31351/vol30iss1pp209-217

Hammodi ID, Abd Alhammid SN (2020) Preparation and characterization of topical letrozole nanoemulsion for breast cancer. Iraqi Journal of Pharmaceutical Sciences 29(1): 195–206. https://doi.org/10.31351/vol29iss1pp195-206

Hejazifar M, Lanaridi O, Bica-Schröder K (2020) Ionic liquid based microemulsions: A review. Journal of Molecular Liquids 303: e112264. https://doi.org/10.1016/j.molliq.2019.112264

Huang YB, Lin YH, Lu TM, Wang RJ, Tsai YH, Wu PC (2008) Transdermal delivery of capsaicin derivative-sodium nonivamide acetate using microemulsions as vehicles. International Journal of Pharmaceutics 349(1–2): 206–211. https://doi.org/10.1016/j.ijpharm.2007.07.022

Jaber SA, Sulaiman HT, Rajab NA (2020) Preparation, characterization and in-vitro diffusion study of different topical flurbiprofen semisolids. International Journal of Drug Delivery Technology 10(1): 81–87. https://doi.org/10.25258/ijddt.10.1.12

Kutscher M, Cheow WS, Werner V, Lorenz U, Ohlsen K, Meinel L, Hadinoto K, Germershaus O (2015) Influence of salt type and ionic strength on self-assembly of dextran sulfate-ciprofloxacin nanoplexes. International Journal of Pharmaceutics 486(1–2): 21–29. https://doi.org/10.1016/j.ijpharm.2015.03.022

Lim, GS, Jaenicke S, Klähn M (2015) How the spontaneous insertion of amphiphilic imidazolium-based cations changes biological membranes: A molecular simulation study. Physical Chemistry Chemical Physics 17(43): 29171–29183. https://doi.org/10.1039/C5CP04806K

Madhav S, Gupta D (2011) A review on microemulsion based system. International Journal of Pharmaceutical Sciences and Research 2(8): 1888–1899. https://doi.org/10.13040/IJPSR.0975-8232

Maraie NK, Almajidi YQ (2018) Application of nanoemulsion technology for preparation and evaluation of intranasal mucoadhesive nano-in-situ gel for ondansetron HCl. Journal of Global Pharma Technology 10(03): 431–442. https://doi.org/10.32947/ajps.v17i2.47

Naeem M (2019) Microemulsion and microemulsion based gel of Zaleplon for transdermal delivery: Preparation, optimization, and evaluation. Acta Poloniae Pharmaceutica-Drug Research 76(3): 543–561. https://doi.org/10.32383/appdr/101663

Nirmala MJ, Allanki S, Mukherjee A, Chandrasekaran N (2013) Enhancing the solubility of fluconazole using a new essential oil based microemulsion system. International Journal of Pharmacy and Pharmaceutical Sciences 5(3): 697–699.

Sabri LA, Sulayman HT, Khalil YI (2009) An investigation release and rheological properties of miconazole nitrate from Emulgel. Iraqi Journal of Pharmaceutical Sciences 18(2): 26–31. https://doi.org/10.31351/vol18iss2pp26-31

Sarheed O, Dibi M, Ramesh KV (2020) Studies on the effect of oil and surfactant on the formation of alginate-based O/W lidocaine nanocarriers using nanoemulsion template. Pharmaceutics 12(12): e1223. https://doi.org/10.3390/pharmaceutics12121223

Simoes MF, Sousa JS, Pais AC (2015) Skin cancer and new treatment perspectives: A review. Cancer Letters 357(1): 8–42. https://doi.org/10.1016/j.canlet.2014.11.001

Sukre M, Barge V, Kasabe A, Shinde T, Kandge M (2022) Formulation and evaluation of econazole nitrate microemulsion. International Journal of Health Scienses 6(S3): 9181–9190. https://doi.org/10.53730/ijhs.v6nS3.8243

Yadav V, Jadhav P, Dombe S, Bodhe A, Salunkhe P (2017) Formulation and evaluation of microsponge gel for topical delivery of antifungal drug. International Journal of Applied Pharmaceutics 9(4): 30–37. https://doi.org/10.22159/ijap.2017v9i4.17760